

## Article

# Removal rates of NO<sub>x</sub>, SO<sub>x</sub>, and fine dust particles in textile fabrics coated with zeolite and coconut shell activated carbon

Keun-Hyeok Yang <sup>1</sup>, Ju-Hyun Mun <sup>2\*</sup> and Jae-Uk Lee <sup>3</sup>

<sup>1</sup> Department of Architectural Engineering, Kyonggi University, Suwon, Kyonggi-do, Republic of Korea; yangkh@kgu.ac.kr

<sup>2</sup> Department of Architectural Engineering, Kyonggi University, Suwon, Kyonggi-do, Republic of Korea; mjh@kgu.ac.kr

\* Correspondence: mjh@kgu.ac.kr; Tel.: +82-(0)31-249-9715

<sup>3</sup> Department of Architectural Engineering, Graduate student, Kyonggi University, Suwon, Kyonggi-do, Republic of Korea; jlee940303@nate.com

**Abstract:** An effective method for coating textile fabrics with porous materials is proposed, and the removal rates of nitrogen oxides (NO<sub>x</sub>), sulfur oxides (SO<sub>x</sub>), and fine dust particles in the coated textile fabrics are evaluated. The textile fabrics made of polyester are used to effectively reduce fine dust particles through static electricity. Zeolite and coconut shell activated carbon are used as porous material to reduce SO<sub>x</sub> and NO<sub>x</sub>, respectively. The effects of the epoxy content and dilution solution types on the SO<sub>x</sub> removal rate of textile fabrics coated with zeolite are evaluated to determine the optimum coating conditions. In addition, the effects of external environmental conditions, such as washing and freeze thawing, on the SO<sub>x</sub> and NO<sub>x</sub> removal rates of the textile fabrics coated with porous materials using the optimum coating conditions are examined. The test results show that the SO<sub>x</sub> removal rate of textile fabrics coated with zeolite decreases with the increase in the epoxy content. The decrease is 2.9 times larger for textile fabrics coated using deionized water than those coated using isopropyl alcohol. After one wash, the SO<sub>x</sub> removal rate decreases dramatically. However, the decrease is reduced by 16% when the epoxy content ratio is increased by 0.5%. The effects of washing and freeze thawing on the SO<sub>x</sub> and NO<sub>x</sub> removal rates of textile fabrics coated using the deionized water diluted with the epoxy content ratio of 2% are minimal. Consequently, to maintain stable SO<sub>x</sub> and NO<sub>x</sub> removal rates under external environmental conditions such as washing and freeze thawing, 98% deionized water dilution and 2% epoxy content ratio are required for the optimum coating of textile fabrics with zeolite and coconut shell activated carbon.

**Keywords:** textile fabric; zeolite; coconut shell activated carbon; NO<sub>x</sub>; SO<sub>x</sub>; fine dust particle

## 1. Introduction

In general, 60% of the fine dust in air is composed of the sulfates or nitrates produced by the combination of exhaust gases, such as sulfur oxides (SO<sub>x</sub>) and nitrogen oxides (NO<sub>x</sub>), with water vapor or ammonia in air [1,2]. Therefore, various efforts have been made to reduce the air pollutants that produce fine dust, particularly in the construction industry [3,4]. Trapalis et al. [3] developed a nano-composite TiO<sub>2</sub> produced from the combination of pure TiO<sub>2</sub> and titanium isopropoxide, and showed that its efficiency in removing NO<sub>x</sub> is better than that of pure TiO<sub>2</sub>. Guo et al. [4] showed that a higher NO<sub>x</sub> removal rate was exhibited in a concrete block coated with TiO<sub>2</sub> compared to that imbedded with TiO<sub>2</sub>. However, most of the existing studies on the removal of air pollutants are based on chemical adsorption by the photocatalyst titanium dioxide (TiO<sub>2</sub>). The adsorption efficiency of TiO<sub>2</sub> in external environmental conditions, such as washing and freeze thawing, is much lower

because  $\text{TiO}_2$  is soluble in water [5]. In addition, the techniques applied in the construction industry have only focused on the removal of  $\text{NO}_x$ , whereas the removal of fine dust particles has received limited attention [6]. Hence, in the construction industry, the techniques for removing stable air pollutants and fine dust particles in external environments required.

Textile fabrics made of polypropylene or polyester formed from fibers with various small diameters are commonly used in the construction industry. Static electricity can be effectively induced by friction in these textile fabrics through rubbing their surfaces. The static electricity can easily cause fine dust particles to adhere to the fabrics owing to the movement of charges. An [7] reported the adsorption of fine dust particles by static electricity in dried polyester fabrics. Kim et al. [8] reported that the fine dust particle removal rate in textile fabrics increased with the applied voltage. Meanwhile, zeolite has a large polarization and effectively forms covalent bonds with  $\text{SO}_x$ , which has dipole moments in ranges similar to that of zeolite [9,10]. Lee et al. [11] studied the reproducibility of the  $\text{NO}_x$  removal rate by zeolite, and reported that the  $\text{NO}_x$  removal rate in zeolite was maintained above 90% throughout 27 times repeats of the experiment. Kopaç and Kocabaş [12] proposed a mechanism for the surface adsorption of  $\text{SO}_2$  on zeolite.

The polarization of coconut shell activated carbon is relatively very low, and effectively forms covalent bonds with  $\text{NO}_x$ , which has dipole moments in similar ranges to that in coconut shell activated carbon [9,13]. In addition, coconut shell activated carbon can physically adsorb  $\text{NO}_x$  because its pore size is similar to movement range of the  $\text{NO}_x$  gas molecules [14]. Park et al. [15] reported that the  $\text{NO}_x$  removal rate of coconut shell activated carbon was improved by 40% after plating the surface of the coconut shell activated carbon with Cu. Lee et al. [16] showed that coconut shell activated carbon with more micropores exhibited a higher  $\text{NO}_x$  removal rate. These results imply that the combination of textile fibers and zeolite or coconut shell activated carbon could be very effective in reducing air pollutants and fine dust particles. Hence, a coating method for textile fibers that maintains a stable air pollutant and fine dust particle removal rate in external environments is required.

The objective of this study is to propose an effective coating method for textile fabrics, and evaluate the removal rates of nitrogen oxides ( $\text{NO}_x$ ), sulfur oxides ( $\text{SO}_x$ ), and fine dust particle in the coated textile fabrics. To effectively reduce the fine dust particles using static electricity, textile fibers made of polyester were used. Zeolite and coconut shell activated carbon were used as porous materials to remove  $\text{SO}_x$  and  $\text{NO}_x$ , respectively. In the coating process, the textile fibers were dipped into a solution of epoxy diluted with deionized water or isopropyl alcohol and combined with the porous materials by a mixer. The effects of the length and density of the uncoated textile fabrics on the removal of fine dust particles were evaluated. In the textile fabrics coated with zeolite, the effects of the epoxy content and the dilution solution type on the  $\text{SO}_x$  removal rate were evaluated and the optimum coating conditions were determined based on these results. In addition, the  $\text{SO}_x$  and  $\text{NO}_x$  removal rates of textile fabrics respectively coated with zeolite and coconut shell activated carbon, using the determined optimum coating conditions were evaluated after washing and freeze thawing to ascertain the removal of stable air pollutants in external environments.

## 2. Research significance

This study proposes textile fibers for building materials that are capable of reducing  $\text{NO}_x$ ,  $\text{SO}_x$ , and fine dust particles by non-electricity based adsorption mechanisms. The optimum coating conditions for the effective coating of the textile fibers with powder-type porous materials diluted with the deionized water or isopropyl alcohol were determined. The air pollutant removal efficiency of the textile fibers coated under the optimum conditions in external environments was evaluated using washing and freeze thawing to simulate the effects of rain and temperature on their efficiency.

## 3. Textile fibers coated with zeolite and coconut shell activated carbon for air pollutant removal

Figure 1 illustrates the proposed idea of using textile fibers for building materials that are capable of reducing  $\text{NO}_x$ ,  $\text{SO}_x$  and fine dust particles. Using epoxy resin and hardener as adhesives, the surfaces of textile fabrics commonly used in the construction industry are coated with porous

materials capable of adsorbing air pollutants. The textile parts of the fabrics adsorb negatively charged fine dust particles through positive charges in the static electricity generated by friction when their surfaces are rubbed together by wind in the external environment (Figure 1a). Zeolite and coconut shell activated carbon were used as porous materials. The zeolite, which has a polarization of  $\delta +$ , attracts and combines with  $\text{SO}_x$ , which has a polarization of  $\delta -$ , via covalent or quadratic bonding (Figure 1b). In addition, coconut shell activated carbon also attracts and combines with  $\text{NO}_x$ , which has a similar polarization to the coconut shell activated carbon, via covalent or quadratic bonding. The coconut shell activated carbon also physically adsorbs  $\text{NO}_x$  because its pore size is similar to the movement range of  $\text{NO}_x$  molecules (Figure 1c). The adsorbed air pollutants and fine dust particles are subsequently washed off from the textile fibers by rain, and after which the porous materials coated on the textile fabrics become capable of re-adsorbing the pollutants again in the external environment without an external electricity supply. These adsorption and washing processes are completely different from the chemical adsorption mechanism in the conventional titanium dioxide ( $\text{TiO}_2$ ) photocatalyst commonly used in building materials.

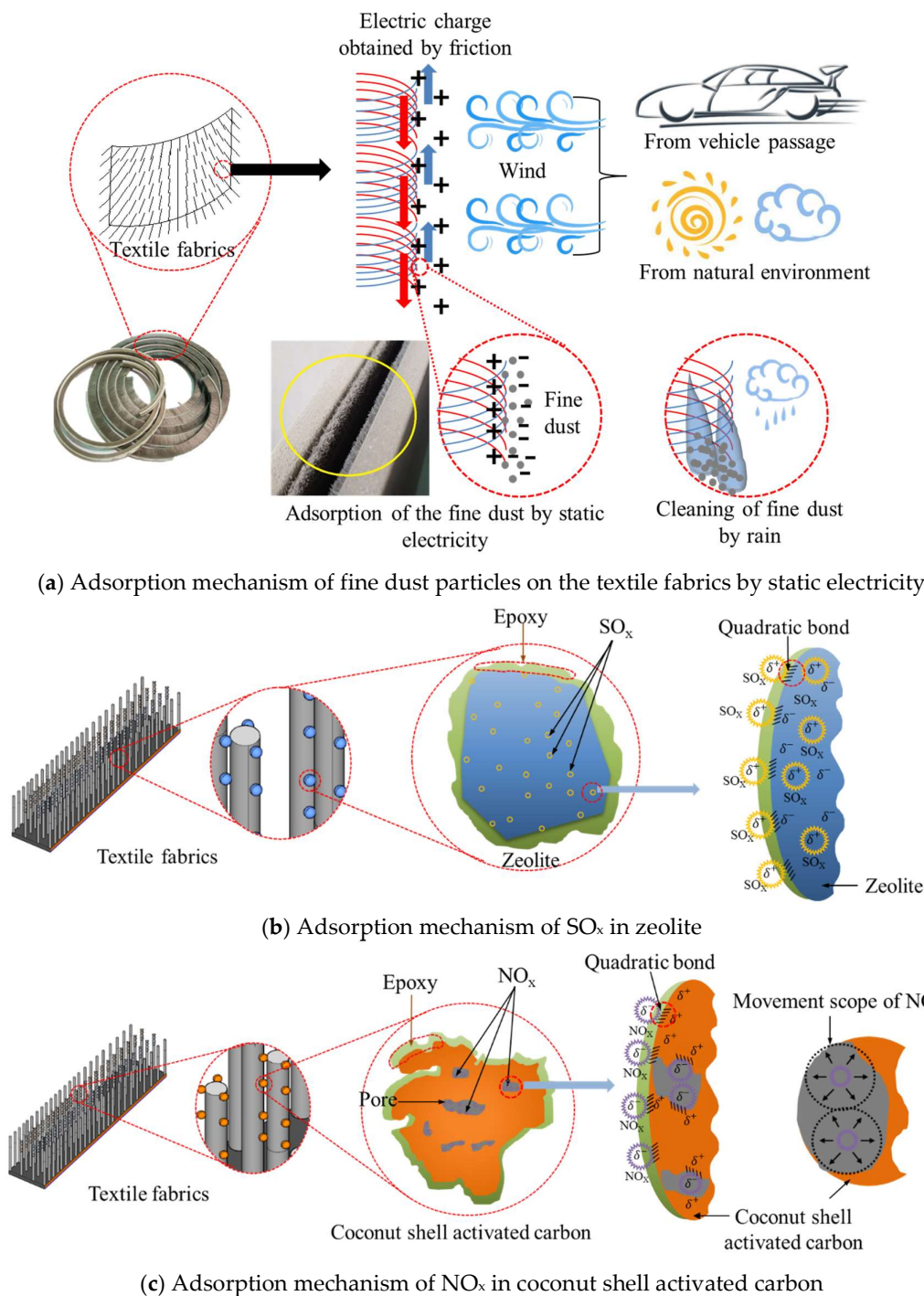
## 4. Experiment

### 4.1. Main parameters

Tables 1 and 2 summarize the main parameters studied in the experiments. The adsorption of fine dust particles by static electricity was investigated in the uncoated textile fabrics. The length and number of layers of uncoated textile fabrics were selected as the main parameters. The length of the uncoated textile fabrics was set as 3.5, 7, or 12 mm, which correspond to the densities of 0.08 g/cm<sup>2</sup>, 0.13 g/cm<sup>2</sup>, and 0.22 g/cm<sup>2</sup>, respectively. The number of layers was set as 4 or 8. Static electricity was introduced into all the textile fabrics artificially by rubbing their top surfaces. In the textile fabrics coated with zeolite, the epoxy content and dilution solution were selected as the main parameters. Additionally, the numbers of washings and freeze-thaw cycles were selected as the main parameters to consider the effects of rain and temperature in the external environment. Deionized water and isopropyl alcohol were used for the dilution solution, and epoxy (resin and hardener) was used as the adhesive. The ratio of the epoxy resin content in the diluted solution was varied from 0 to 2%. The number of washings was set to 0, 1, or 10, and the number of freeze-thaw cycles to 0 and 1 cycle. The number of washings and freeze-thaw cycles used for the textile fabrics coated with coconut shell activated carbon were identical to those selected for textile fabrics coated with zeolite. The optimum epoxy content and solution determined from the coating process of zeolite were used for the coating the textile fibers with coconut shell activated carbon.

### 4.2. Materials


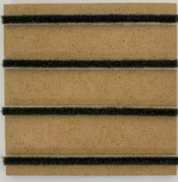





Table 3 summarizes the physical properties of the porous materials used. The textile fabrics were made of polyester, and their length and fiber diameter were 15 mm and 20  $\mu\text{m}$ , respectively. The sizes of the zeolite particles were between 3 and 10  $\mu\text{m}$ , and the density of zeolite was 2.37 g/cm<sup>3</sup>. The sizes of the coconut shell activated carbon particles were between 5 and 10  $\mu\text{m}$ , and the density of the coconut shell activated carbon was 1.56 g/cm<sup>3</sup>. The density of hardened epoxy resin was 1.18 g/cm<sup>3</sup> and its hardness was 83 Shore D. Figure 2 shows the distributions of the pore sizes and images of the internal pores in the porous materials. Pore sizes ranging between 0.4 and 185 nm was measured using the Brunauer-Emmett-Teller (BET) technique, while pore sizes larger than 185 nm were measured using mercury intrusion porosimetry. The internal microstructure was analyzed from the scanning electron microscopy (SEM) images. As shown in Figure 2a, the textile fibers had cylindrical shapes and were intertwined. The micropores, mesopores, and macropores respectively constituted



**Figure 1.** The textile fabrics coated with porous materials for reducing air pollutants.

7.4, 2.7, and 89.9% of the pores in zeolite, indicating that most of the pores in zeolite were larger than  $0.05 \mu\text{m}$ . As shown in Figure 2b, the internal structure of zeolite consisted of irregular polygons. The micropore, mesopore, and macropore distribution in coconut shell activated carbon were 74.7, 9.7, and 15.6%, respectively, indicating that the most common pore size in zeolite was the micropore, which is similar to the range of molecular movement in  $\text{NO}_x$  [14]. In addition, the internal structure of the coconut shell activated carbon had many pores of various diameters (Figure 2c). The micropore, mesopore, and macropore distribution of hardened epoxy were 15.0, 2.7, and 85.3%, respectively,

**Table 1.** Main parameters for evaluating the fine dust particle removal rate of the textile fabric specimens.

| Specimen | Length (mm) | Layers | Density (g/cm <sup>2</sup> ) | Details   |
|----------|-------------|--------|------------------------------|---|
| F-C      | -           | -      | -                            |    |
| F-3.5-4  | 3.5         | 4      | 0.08                         |    |
| F-3.5-8  | 3.5         | 8      | 0.08                         |    |
| F-7.0-4  | 7           | 4      | 0.13                         |  |
| F-7.0-8  | 7           | 8      | 0.13                         |  |
| F-12-4   | 12          | 4      | 0.22                         |  |
| F-12-8   | 12          | 8      | 0.22                         |  |

indicating that the most common pore size in epoxy was the macropore, which is 5.7 times larger than the molecular movement range of SO<sub>x</sub> and NO<sub>x</sub>.

**Table 2.** Main parameters for evaluating the NO<sub>x</sub> and SO<sub>x</sub> removal rates of the textile fabric specimens.

| Specimens  | Porous material type           | Solution type      | Epoxy contents (%) | Number of washings | Number of freezing-thaw cycles |
|------------|--------------------------------|--------------------|--------------------|--------------------|--------------------------------|
| Z-W-0-0    | Zeolite                        | DI                 | 0                  | 0                  | 0                              |
| Z-W-0-1    |                                |                    |                    | 1                  | 0                              |
| Z-W-1-0    |                                |                    | 1                  | 0                  | 0                              |
| Z-W-1-1    |                                |                    |                    | 1                  | 0                              |
| Z-W-1.5-0  |                                |                    | 1.5                | 0                  | 0                              |
| Z-W-1.5-1  |                                |                    |                    | 1                  | 0                              |
| Z-W-2-0    |                                |                    | 2                  | 0                  | 0                              |
| Z-W-2-1    |                                |                    |                    | 1                  | 0                              |
| Z-W-2-10   |                                |                    |                    | 10                 | 0                              |
| Z-W-2-10-F |                                |                    |                    | 10                 | 1                              |
| Z-A-0-0    | Zeolite                        | IPA                | 0                  | 0                  | 0                              |
| Z-A-0-1    |                                |                    |                    | 1                  | 0                              |
| Z-A-1-0    |                                |                    | 1                  | 0                  | 0                              |
| Z-A-1-1    |                                |                    |                    | 1                  | 0                              |
| Z-A-2-0    |                                |                    | 2                  | 0                  | 0                              |
| Z-A-2-1    |                                |                    |                    | 1                  | 0                              |
| Z-WA-1-0   | Zeolite                        | 90% DI and 10% IPA | 1                  | 0                  | 0                              |
| Z-WA-1-1   |                                |                    |                    | 1                  | 0                              |
| Z-WA-2-0   |                                |                    | 2                  | 0                  | 0                              |
| Z-WA-2-1   |                                |                    |                    | 1                  | 0                              |
| C-W-2-0    | Coconut shell activated carbon | DI                 | 2                  | 0                  | 0                              |
| C-W-2-1    |                                |                    |                    | 1                  | 0                              |
| C-W-2-10   |                                |                    |                    | 10                 | 0                              |
| C-W-2-10-F |                                |                    |                    | 10                 | 1                              |

DI and IPA refer to deionized water and isopropyl alcohol, respectively.

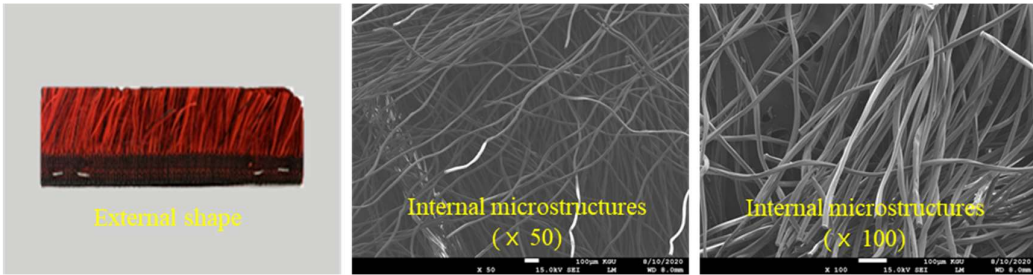
**Table 3.** Physical properties of porous materials.

| Type                           | Particle size (μm) | Density (g/cm <sup>3</sup> ) | Fineness (m <sup>2</sup> /g) |
|--------------------------------|--------------------|------------------------------|------------------------------|
| Zeolite                        | 3 – 10             | 2.37                         | 2.3                          |
| Coconut shell activated carbon | 5 – 10             | 1.56                         | 1130.1                       |

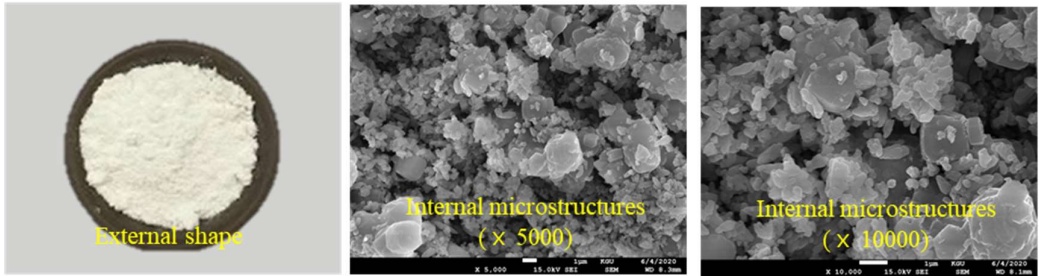
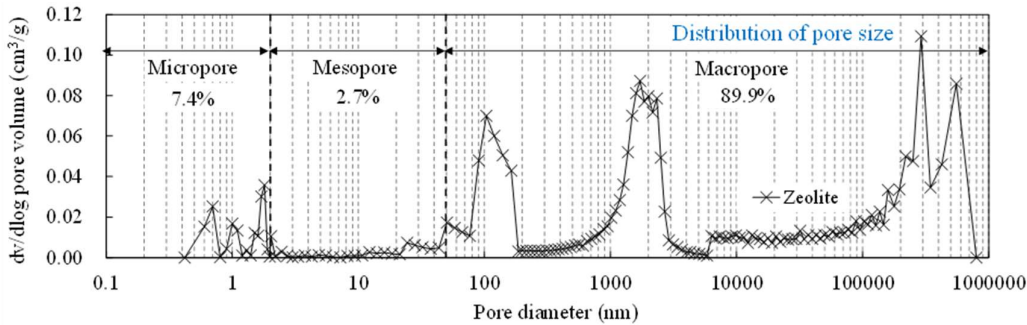
#### 4.3. Coating method of porous materials on textile fibers

Figure 3 shows the coating method of zeolite or coconut shell activated carbon and the epoxy on the textile fibers. The considerably high viscosity of epoxy results in a high possibility of forming

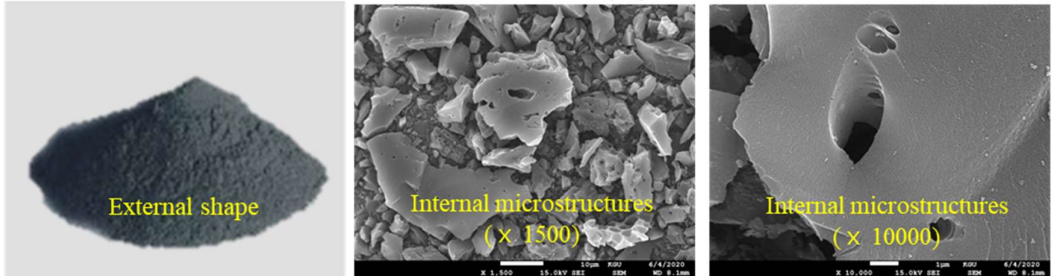
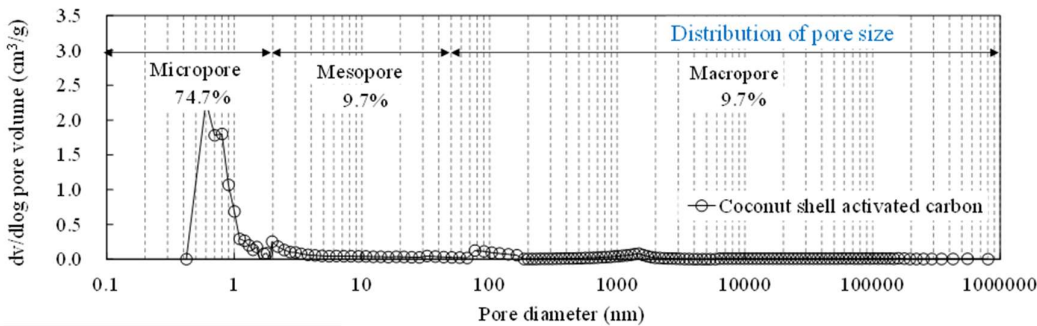




(a) Textile fabrics



(b) Zeolite



(c) Coconut shell activated carbon

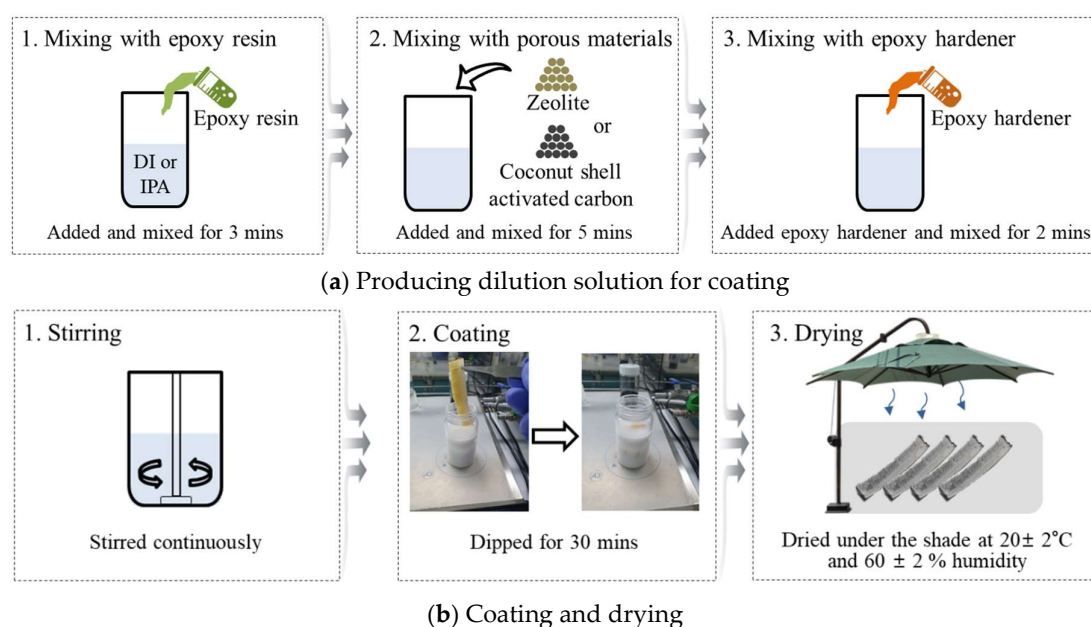
Figure 2. Internal microstructure and pore distribution of each material used.

entangled lumps with the zeolite or coconut shell activated carbon powder [17]. Hence, to reduce the formation of entangled lumps, the epoxy needs to be diluted to a high-flow solution [18]. As shown in Figure 3, the deionized water or isopropyl alcohol for dilution was mixed with the epoxy resin for 3 min. Subsequently, the zeolite or coconut shell activated carbon powder was added and mixed for 5 min. The epoxy hardener was finally added and mixed for 2 min. The textile fibers were fully dipped into the combined dilution solution and stirred continuously. The dipping time was 30 min. The dipped textile fibers were dried under a shade at  $20 \pm 2$  °C and  $60 \pm 2\%$  humidity.

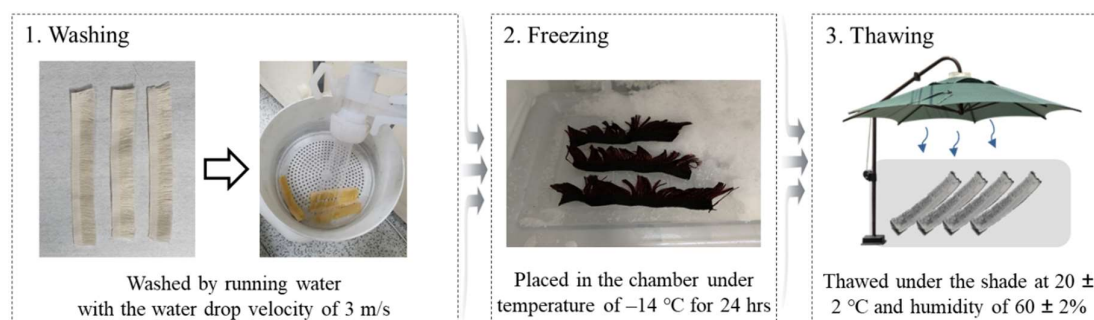
#### 4.4. Experimental procedures

Figure 4 shows the washing and freeze-thawing process of the textile fibers coated with porous materials. In the washing process, the textile fibers coated with porous materials were washed by running water with the water drop velocity of 3 m/s, which is the maximum water velocity in rain. In the freeze thawing process, the textile fibers were placed in a chamber with a temperature below  $-14$  °C for 24 h after washing, and then thawed under the shade at  $20 \pm 2$  °C and  $60 \pm 2\%$  humidity. Before testing, the processed textile fibers were dried under the shade.

The fine dust particles on the textile fibers were measured using a machine that counted the number of fine dust particles with a laser [19]. As shown in Figure 5a, the counting machine comprised a laser counter, a chamber, and a fan. The octagonal chamber had a dimension of  $405 \times 405 \times 120$  mm. The dimension of the textile fabrics specimen was  $115 \times 115 \times 10$  mm. The fabrics was



**Figure 3.** Coating method of the textile fabrics.

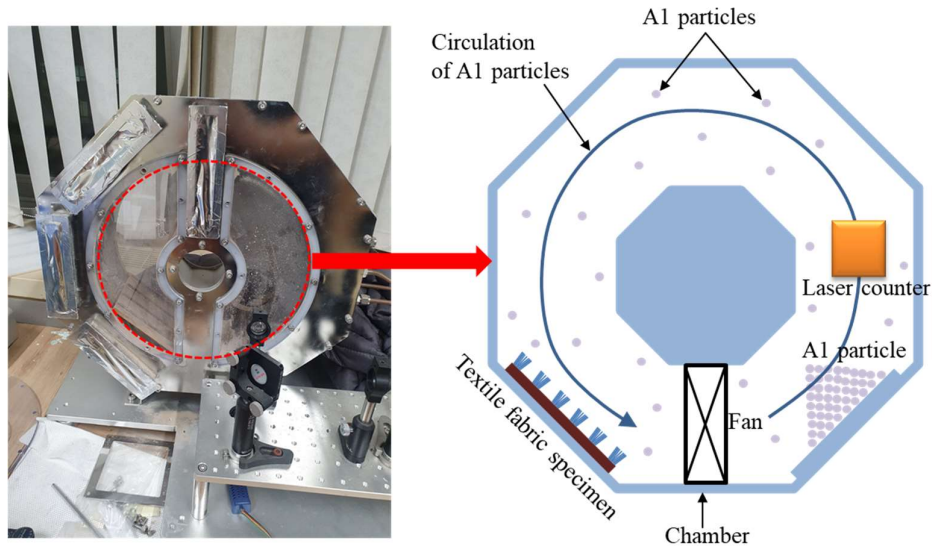


**Figure 4.** Washing and freeze-thaw process of the textile fabrics with porous materials.

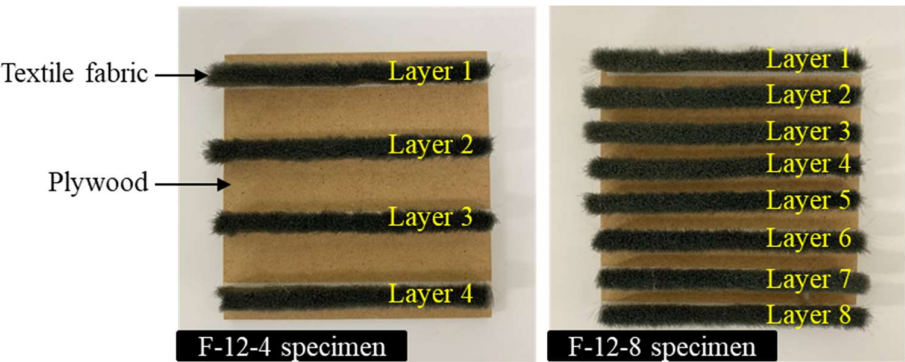


attached onto plywood, which is not considerably affected by the static electricity, to fix it in the chamber (Figure 5b). To circulate the fine dust particles in the chamber, the fan was operated with a constant wind velocity of approximately 9.78 m/s during the experiment. The variation of the number of fine dust particles with respect to time was measured by counting the fine dust particles reflected by the laser. The fine dust particles used was A1 ultrafine test dust (ISO 12103-1, Arizona Test Dust), which is commonly used for the testing air purification filters [20]. The sizes of most of the A1 dust particles ranged between 0.97 and 5.5  $\mu\text{m}$ , which is similar to that of the ultrafine dust particles (2.5 PM) in the air [20]. Most of the A1 dust was circulated continuously by the airflow generated from the fan, whereas only some dust was attached to the chamber. Because the number of fine dust particles decreased even without the textile fibers in the chamber, the number of fine dust particles obtained from the chamber containing the textile fabric specimen was compared with that without the textile fabric specimen.

Figure 6 shows the measurement machine for the removal of  $\text{SO}_x$  and  $\text{NO}_x$  by the textile fabrics coated with the porous materials. The measurement machine was composed of a chamber, a velocity and flow controller, a gas inlet and outlet, and a gas analyzer. The chamber had shape of a rugby ball with a 90 mm inner diameter and 178 mm length. The textile fabric specimen was placed on the circular platform in the center of the chamber.  $\text{SO}_x$  or  $\text{NO}_x$  gas was then injected using the velocity and flow controller, and the decrease in the gas concentration in the chamber with the coated textile

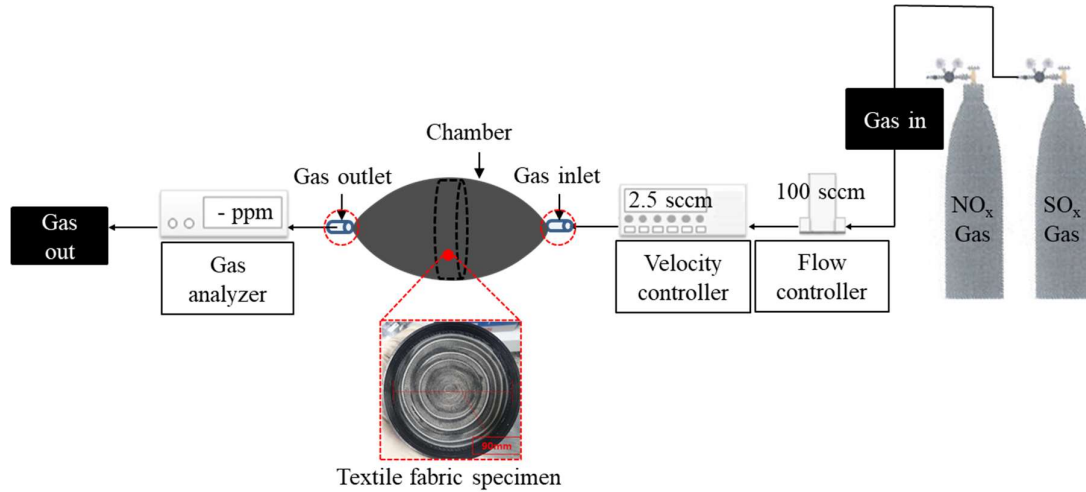


(a) Schematic of machine for counting the fine dust particles



(b) Details of textile fabric specimens

**Figure 5.** Test setup for measuring fine dust particle removal rates.

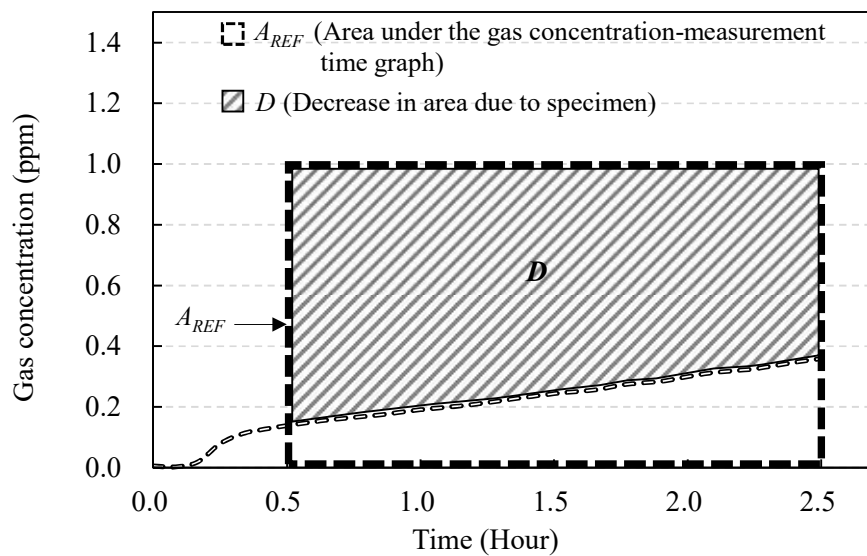


**Figure 6.** Machine for measuring  $\text{SO}_x$  and  $\text{NO}_x$  removal by the textile fabric.

fabric specimen was measured using the gas analyzer connected to the gas outlet. The injection velocity and flow content were determined by the values required for maintaining a gas concentration of 1 ppm in the chamber without the specimen. The  $\text{SO}_x$  or  $\text{NO}_x$  removal rate of the coated textile fabric specimen was evaluated by comparing the variation of the gas concentration in the chamber with and without the specimen. In accordance with ISO 22197-1 [21], the  $\text{SO}_x$  or  $\text{NO}_x$  removal rate was calculated as follows:

$$R_{air} = \frac{D}{A_{REF}} \times 100 \quad (1)$$

where  $A_{REF}$  is the area under the graph of the variation of the gas concentration with respect to the time in the chamber, and  $D$  is the decrease in the graph area of the  $\text{SO}_x$  or  $\text{NO}_x$  concentration due to the specimen (Figure 7). The microstructures and compositions of the textile fabrics coated with zeolite and coconut shell activated carbon were examined using SEM and energy dispersive X-ray spectroscopy (EDS) using an electron microscope.



**Figure 7.** Variation of gas concentration with respect to time.

## 5. Results and discussion

### 5.1. Effect of length and density of textile fabrics

Figure 8 shows the number of A1 particles with respect to the time. The decrease in the number of A1 particles obtained from the chamber without a specimen was less than 17% in the first 20 min. The decrease dramatically increased after that. The decrease at 30 min was approximately 78%. The point in time at which the decrease began to increase dramatically and the decrease became more notable occurred earlier as the length and density of the textile fabrics increased. The number of A1 particles dramatically decreased at 12 min for the specimen with 3.5 mm length and 4 layers, and at 7 min for the specimen with 12 mm length and 4 layers.

The time at which the number of A1 particles reached zero was 29 min for the specimen with 3.5 mm length and 4 layers, and 26 min for the specimen with 3.5 mm length and 8 layers. The corresponding values were 25 min for the specimen with 12 mm length and 4 layers, and 22 min for the specimen with 12 mm length and 8 layers. Table 4 summarizes the results for the number of A1 particles. Because of the large scatter observed in the number of A1 particles with respect to time, the

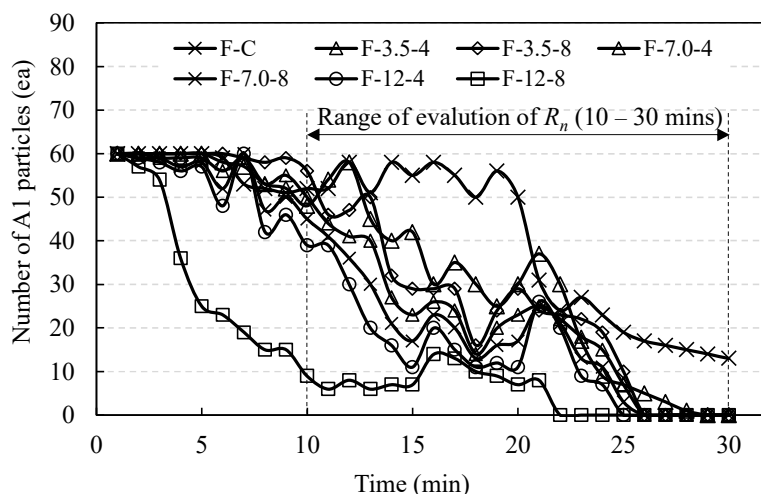


Figure 8. Number of A1 particles with respect to time.

Table 4. Summary of the number of A1 particles adsorbed on the textile fabrics.

| Specimens | Removal rate of A1 particles at termination of test (%) | Time which the number of A1 particles reached zero (min) | $R_n$ (%) |
|-----------|---|--|-----------|
| F-C       | 77.5  | -  | -         |
| F-3.5-4   | 100   | 29   | 20        |
| F-3.5-8   | 100   | 26   | 21        |
| F-7.0-4   | 100   | 26   | 23        |
| F-7.0-8   | 100   | 25   | 33        |
| F-12-4    | 100   | 25   | 36        |
| F-12-8    | 100   | 22   | 52        |

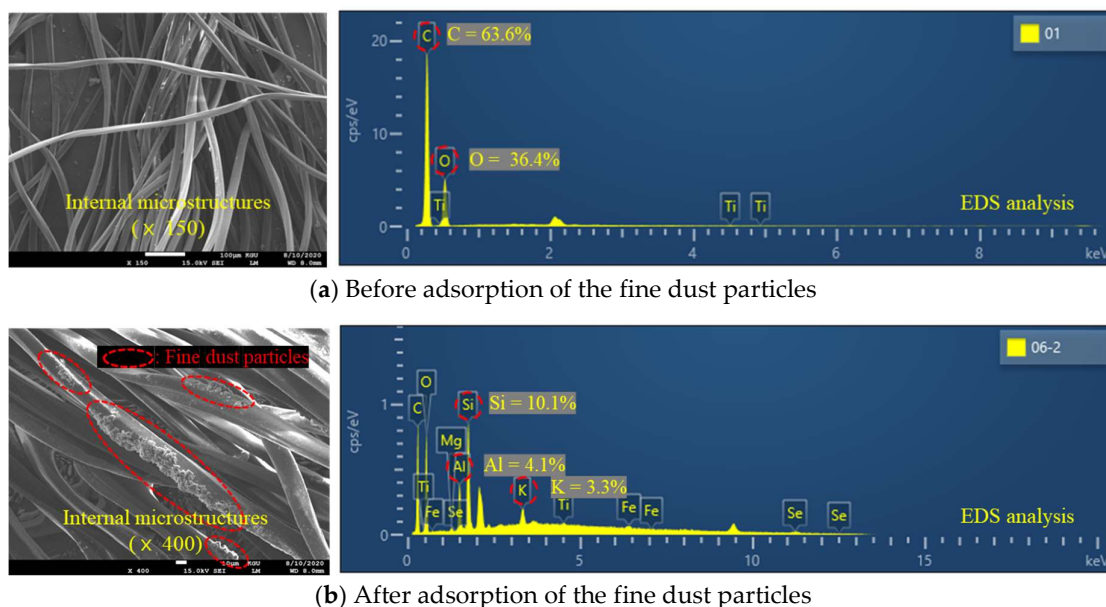
$R_n$  = The ratio of the number of A1 particles obtained from the chamber with specimen to that without specimen between 10 and 30 min.

fine dust particle removal rate was evaluated by comparing the ratios ( $R_n$ ) of the number of A1 particles obtained from the chamber with the specimen to that without the specimen between 10 and 30 min when the number of A1 particles decreased dramatically. The results are shown in Figure 8, At the end of the test, approximately 77.5% of the A1 particles were removed from the chamber without a specimen whereas all the particles were removed from the chamber with a specimen. Between 10 and 30 min, the  $R_n$  value increased with the length of the textile fibers, indicating that the increase was more notable for the specimens with denser textile fibers. The  $R_n$  of the specimen with 12 mm length and 4 layers is 1.8 times higher than that with 3.5 mm length and 4 layers. In addition, the  $R_n$  of the specimen with 12 mm length and 8 layers arrangement is 2.47 times higher than that with 3.5 mm length and 8 layers.

Figure 9 shows the SEM image and EDS spectra of the textile fibers before and after adsorbing the fine dust particles. Before adsorbing the fine dust particles, C and O were present at the proportions of 63.6% and 36.4%, respectively. After adsorbing the fine dust particles, the additional presence of 10.1% Si, 4.1% Al, and 3.3% K was observed. This implies that the definite adsorption of the fine dust particles on the surface of the textile fabrics because Si and Al are the main components of the fine dust particles. The adsorption of the fine dust particles was also confirmed from the SEM image.

### 5.2. Effect of epoxy content and dilution solution on $\text{SO}_x$ removal rate

As summarized in Table 5, the  $\text{SO}_x$  removal rate decreased with the increase in the epoxy content, indicating that the decrease was affected by the solution type. The  $\text{SO}_x$  removal rate of the coated textile fabrics using deionized water as the dilution solution decreased by approximately 7% when the epoxy contents increased from 0% to 2%. The  $\text{SO}_x$  removal rate of the coated textile fibers using isopropyl alcohol as the dilution solution decreased by approximately 20%, which is approximately 2.8 times the decrease when deionized water was used as the dilution solution. In addition, the  $\text{SO}_x$  removal rate of the coated textile fibers using the combination of 90% deionized water and 10% isopropyl alcohol as the dilution solution decreased by approximately 8.9%, when the epoxy contents increased from 1% to 2%. This implies that the use of deionized water for the dilution solution is more effective for alleviating the decrease in the  $\text{SO}_x$  removal rate with the increase in epoxy contents than the use of isopropyl alcohol.



**Figure 9.** SEM images and EDS spectra of the uncoated textile fibers.

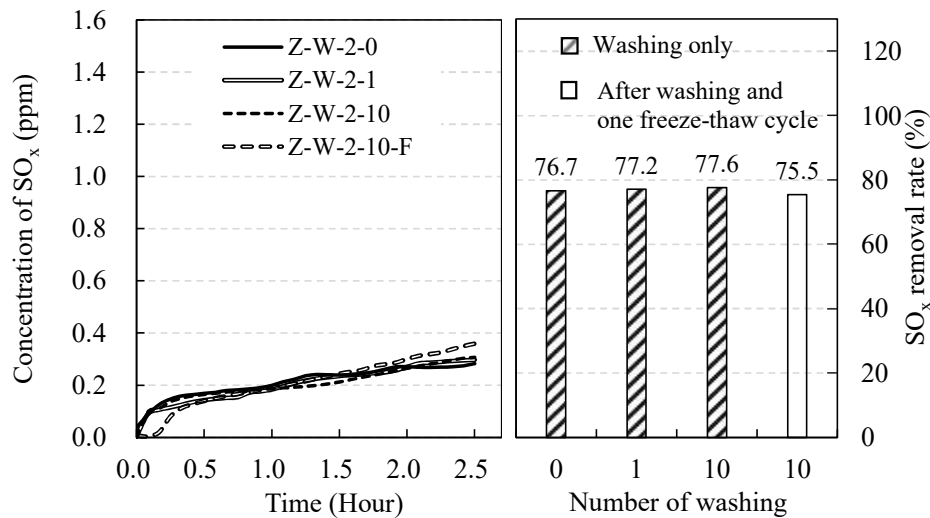


**Table 5.** Summary of the SO<sub>x</sub> and NO<sub>x</sub> removal rates of textile fabrics coated with zeolite or coconut shell activated carbon.

| Specimens  | Porous material type | Solution type      | Epoxy mixing ratio (%) | Number of washings | Number of freezing-thaw cycles | Removal rate (%) |                 |
|------------|----------------------|--------------------|------------------------|--------------------|--------------------------------|------------------|-----------------|
|            |                      |                    |                        |                    |                                | SO <sub>x</sub>  | NO <sub>x</sub> |
| Z-W-0-0    | Zeolite              | DI                 | 0                      | 0                  | 0                              | 83.4             | -               |
| Z-W-0-1    |                      |                    |                        | 1                  | 0                              | 34.9             | -               |
| Z-W-1-0    |                      |                    | 1                      | 0                  | 0                              | 74.7             | -               |
| Z-W-1-1    |                      |                    |                        | 1                  | 0                              | 66.2             | -               |
| Z-W-1.5-0  |                      |                    | 1.5                    | 0                  | 0                              | 68.3             | -               |
| Z-W-1.5-1  |                      |                    |                        | 1                  | 0                              | 60.8             | -               |
| Z-W-2-0    |                      |                    | 2                      | 0                  | 0                              | 76.7             | -               |
| Z-W-2-1    |                      |                    |                        | 1                  | 0                              | 77.2             | -               |
| Z-W-2-10   |                      |                    |                        | 10                 | 0                              | 77.6             | -               |
| Z-W-2-10-F |                      |                    |                        | 10                 | 1                              | 75.5             | -               |
| Z-A-0-0    | Zeolite              | IPA                | 0                      | 0                  | 0                              | 86.3             | -               |
| Z-A-0-1    |                      |                    |                        | 1                  | 0                              | 26.6             | -               |
| Z-A-1-0    |                      |                    | 1                      | 0                  | 0                              | 84.7             | -               |
| Z-A-1-1    |                      |                    |                        | 1                  | 0                              | 58.8             | -               |
| Z-A-2-0    |                      |                    | 2                      | 0                  | 0                              | 66.1             | -               |
| Z-A-2-1    |                      |                    |                        | 1                  | 0                              | 62.4             | -               |
| Z-WA-1-0   | Zeolite              | 90% DI and 10% IPA | 1                      | 0                  | 0                              | 90.6             | -               |
| Z-WA-1-1   |                      |                    |                        | 1                  | 0                              | 73.4             | -               |
| Z-WA-2-0   |                      |                    | 2                      | 0                  | 0                              | 81.7             | -               |
| Z-WA-2-1   |                      |                    |                        | 1                  | 0                              | 74.8             | -               |
| C-W-2-0    | Coconut              | DI                 | 2                      | 0                  | 0                              | -                | 19.8            |
| C-W-2-1    | shell                |                    |                        | 1                  | 0                              | -                | 16.9            |
| C-W-2-10   | activated            |                    |                        | 10                 | 0                              | -                | 16.6            |
| C-W-2-10-F | carbon               |                    |                        | 10                 | 1                              | -                | 16.3            |

### 5.3. Effect of external environment on SO<sub>x</sub> removal rate

Figure 10 show the SO<sub>x</sub> removal rate of the textile fibers coated with zeolite after exposure to the external environment. After one washing, the SO<sub>x</sub> removal rate dramatically decreased. The decrease was 52.5% at 2% epoxy content. The lowest SO<sub>x</sub> removal rate in the textile fibers using deionized water as the dilution solution was 34.9% at the epoxy content of 0%. The removal rate was 77.2% at the epoxy content of 2%, which is 2.2 times higher than that at the epoxy content of 0%. After 10 washings, the SO<sub>x</sub> removal rate of the coated textile fibers using deionized water as the dilution solution was 77.6% at 2% epoxy content. In addition, after 10 washings and a single freeze-thaw cycle, The removal rate was 75.5%, which is similar to that before exposure to the external environmental conditions of washing and freeze thawing. Meanwhile, the SO<sub>x</sub> removal rate of the coated textile fibers using isopropyl alcohol as the dilution solution after one washing exhibited similar trends to the removal rate using deionized water as the dilution solution. After one washing, the SO<sub>x</sub> removal rate of the coated textile fibers using isopropyl alcohol as the dilution solution was 26.6% at the epoxy content of 0%, and 62.4% at the epoxy content of 2%. This implies that a higher epoxy content is effective in maintaining a stable SO<sub>x</sub> removal rate in external environmental conditions such as



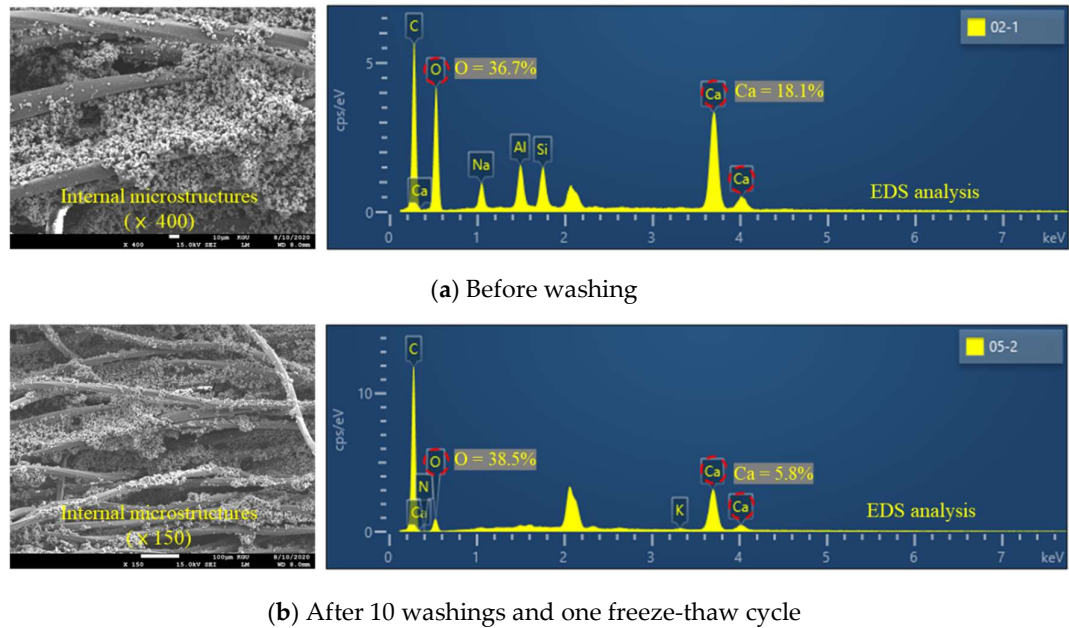
**Figure 10.** SO<sub>x</sub> removal rate of textile fabrics coated with zeolite after exposure to external environmental conditions.

washing or freeze thawing, because the epoxy directly affects the degree of adhesion between the textile fabrics and the zeolite.

Figure 11 shows the SEM image and EDS spectra of the textile fabrics coated with zeolite. As shown in Figure 11a, before washing, O and Ca, which are the main components of zeolite, were present in the coated fabric in the proportions of 36.7% and 18.1%, respectively. After 10 washings and one freeze-thaw cycle, the proportions of O and Ca were 38.5% and 5.8%, respectively. This implies that the zeolite was well attached to the surface of the textile fabrics after exposure to external environmental condition such as washing or freeze thawing. The attachment of the zeolite to the fabrics was also confirmed in the SEM image in Figure 11b.

5.4. Effect of external environment condition on NO<sub>x</sub> removal rate

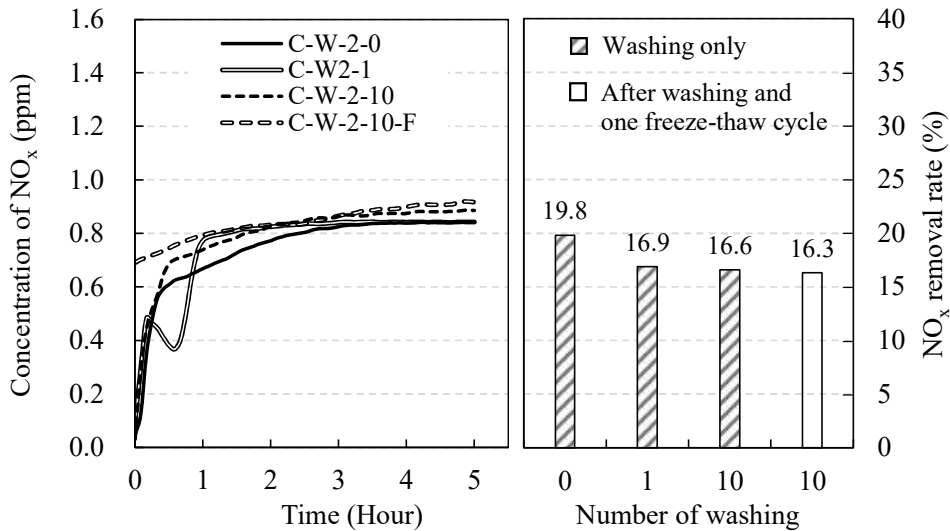
Based on the results obtained from sections 5.2 and 5.3, the textile fibers were coated with



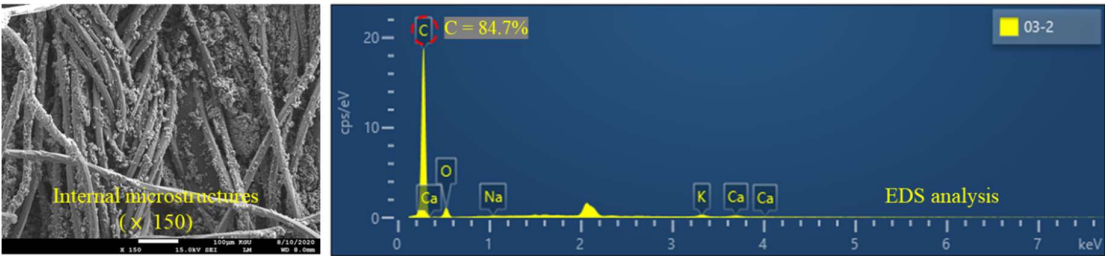
**Figure 11.** SEM images and EDS spectra of textile fabric coated with zeolite.

coconut shell activated carbon using 98% deionized water for the dilution solution and 2% epoxy. Figure 12 show the NO<sub>x</sub> removal rate of the textile fibers coated with coconut shell activated carbon after exposure to external environmental conditions. The washing and freeze thawing procedures were identical to those in section 5.3. Before washing, the NO<sub>x</sub> removal rate was 19.8%. This value was maintained after one and after 10 washings in which the removal rates were 16.9% and 16.6%, respectively. In particular, after 10 washings and one freeze-thaw cycle, the NO<sub>x</sub> removal rate was 16.3%, which is similar to that after one washing. This implies that the coating conditions of the solution type and epoxy content determined from the coating procedure of textile fibers with zeolite are effective in maintaining a stable NO<sub>x</sub> removal rate in textile fibers coated with coconut shell activated carbon in external environments.

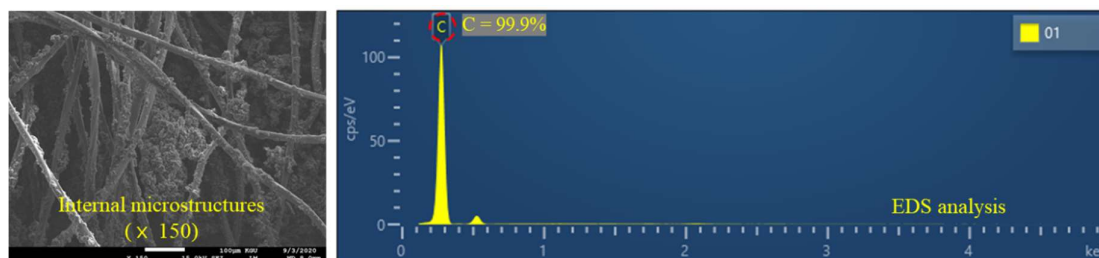
Figure 13 shows the SEM image and EDS spectra of the textile fibers coated with coconut shell activated carbon. As shown in Figure 13a, before washing, C, which is the main components of coconut shell activated carbon, was present at the proportion of 84.7%. After 10 washings and one freeze-thaw cycle, the proportion of C was 99.9%. This implies that the coconut shell activated carbon was well attached to the surface of the textile fabrics after exposure to external environmental conditions such as washing or freeze thawing. The attachment of the coconut shell activated carbon wwwwwwwwwis also confirmed in the SEM image in Figure 13b.



**Figure 12.** NO<sub>x</sub> removal rate of textile fabrics coated with coconut shell activated carbon after exposure to external environmental conditions.



(a) Before washing



(b) After 10 washing and one freeze-thaw cycle

**Figure 13.** SEM images and EDS spectra of the uncoated textile fibers.

## 6. Conclusions

An effective method for coating textile fabrics with porous materials was proposed, and the air pollutant removal rates of the textile fabrics after exposure to external environments were evaluated. The conclusions drawn are as follows:

- The removal rate of fine dust particles increased by 1.8 and 2.47 times, respectively, for textile fibers with 4 and 8 layers when the length of the textile fabric increased from 2.5 to 12 mm.
- The sulfur oxides ( $\text{SO}_x$ ) removal rate of the textile fabrics coated with zeolite decreased with the increase in the epoxy content ratio. The decrease in the textile fabrics using isopropyl alcohol as the dilution solution was 23.4%, which is 2.9 times higher than in the textile fabrics using deionized water as the dilution solution.
- After one washing, the textile fabrics coated with zeolite without using epoxy had the lowest  $\text{SO}_x$  removal rate of 26.6%, whereas the corresponding values using an epoxy content of 2% and deionized water or isopropyl alcohol for the dilution solution were 77.2 and 62.4%, respectively, which are similar to the values before washing.
- After 10 washings and one freeze-thaw cycle, the  $\text{SO}_x$  and nitrogen oxides ( $\text{NO}_x$ ) removal rates of the coated textile fibers using deionized water and the epoxy contents of 2% were 75.5 and 16.3%, respectively, similar to those after one washing.
- In the coated textile fibers before washing or freeze thawing, the proportions of O and C, which are the main components of zeolite and coconut shell activated carbon, were 36.7 and 84.7%, respectively. These values are similar to those for the coated textile fibers exposed to 10 washings and one freeze-thaw cycle.
- To maintain stable  $\text{SO}_x$  and  $\text{NO}_x$  removal rates in the textile fabrics exposed to external environmental conditions such as washing and freeze thawing, 98% deionized water for the dilution solution and 2% epoxy content are required for the optimum coating of the textile fibers with zeolite and coconut shell activated carbon.

**Author Contributions:** K.-H.Y. designed project. J.-H.M. and J.-U.L. conducted the analysis of test results obtained this study. All authors contributed to the comprehensive analysis and conclusion.

**Funding:** This research was funded by the Korea Institute of Energy Technology Evaluation and Planning (KETEP) and the Ministry of Trade, Industry & Energy (MOTIE) of the Republic of Korea.

**Acknowledgments:** This work was supported by the Korea Institute of Energy Technology Evaluation and Planning (KETEP) and the Ministry of Trade, Industry & Energy (MOTIE) of the Republic of Korea (No. 20181110200070).

**Conflicts of Interest:** The authors declare no conflict of interest.

## References

1. Jiang, K.; Yu, H.; Chen, L.; Fang, M.; Azzi, M. An advanced, ammonia-based combined  $\text{NO}_x/\text{SO}_x/\text{CO}_2$  emission control process towards a low-cost, clean coal technology. *Applied Energy* **2020**, *260*, 1–12.
2. Yu, H.; Morgan, S.; Allport, A.; Do, T.; Cottrell, A.; McGregor, J. Update on aqueous ammonia based post combustion capture pilot plant at Munmorah. *Distillation Absorption* **2010**, *NL*, 115–120.



3. Trapalis, A.; dk Giannakopoulou, T.; Boukos, N.; Speliotis, T.; Dimotikali, D.; Yu, J. TiO<sub>2</sub>/graphene composite photocatalysts for NO<sub>x</sub> removal: A comparison of surfactant-stabilized graphene and reduced graphene oxide. *Applied Catalysis B: Environmental* **2016**, *180*, 637–647.
4. Guo, M.Z.; Ling, T.C.; Poon, C. S. Photocatalytic NO<sub>x</sub> degradation of concrete surface layers intermixed and spray-coated with nano-TiO<sub>2</sub>: Influence of experimental factors. *Cement and Concrete Composites* **2017**, *83*, 279–289.
5. Dylla, H.; Hassan, M.M.; Schmitt, M.; Rupnow, T.; Mohammad, L.M. Laboratory investigation of the effect of mixed nitrogen dioxide and nitrogen oxide gases on titanium dioxide photocatalytic efficiency in concrete pavements. *Journal of Materials in Civil Engineering* **2010**, *23*, 1087–1093.
6. Yoon, I.H.; Lee, K.B.; Kim, J.S.; Kim, S.D. A study on the estimation of NO<sub>x</sub> reduction in ambient by photocatalyst (TiO<sub>2</sub>) block. *Journal of the Korean Society of Urban Environment* **2017**, *17*, 433–443.
7. An, E.J. A study of dyeing polyester fiber using alkali treatment. *Journal of Basic Design & Art* **2014**, *15*, 185–194.
8. Chatterjee, K.N.; Mukhopadhyay, A.; Jhalani, S.C.; Mani, B.P. Performance characteristics of filter fabrics in cement dust control: Part II-Influence of fibre cross-sectional shape and scrim on the performance of nonwoven filter fabrics. *Indian Journal of Fibre & Textile Research* **1996**, *21*, 251–260.
9. Wang, Z.; Guo, M.; Mu, X.; Sen, S.; Insley, T.; Mason, A.J.; Král, P.; Zeng, X. Highly sensitive capacitive gas sensing at ionic liquid–electrode. *Analytical Chemistry* **2016**, *88*, 1959–1964.
10. Kopaq, T.; Kaymakgi, E.; Kopac, M. Dynamic adsorption of SO<sub>2</sub> on zeolite molecular sieves. *Chemical Engineering Communications* **1998**, *164*, 99–109.
11. Lee, S.J.; Shin, C.S.; Lee, T.H. Removal and regeneration of SO<sub>2</sub> by cupric oxide supported on zeolite. *Journal of Korean Society for Atmospheric Environment* **1990**, *6*, 161–167.
12. Kopaç, T.; Kocabaş, S. Sulfur dioxide adsorption isotherms and breakthrough analysis on molecular sieve 5A zeolite. *Chemical Engineering Communications* **2010**, *190*, 1041–1054.
13. Chiang, Y.C.; Chiang, P.C.; Chang, E.E. Effects of surface characteristics of activated carbons on VOC adsorption. *Journal of Environmental Engineering* **2001**, *127*, 54–62.
14. Al-Rahbi, A.S.; Williams, P.T. Production of activated carbons from waste tyres for low temperature NO<sub>x</sub> control. *Waste Management* **2016**, *49*, 188–195.
15. Park, S.J.; Kim, B.J.; Kawasaki, J. NO removal of electrolessly copper-plated activated carbons. *HWAHAK KONGHAK* **2003**, *41*, 795–801.
16. Lee, S.W.; Bae, S.K.; Kwon, J.H.; Na, Y.S.; An, C.D.; Yoon, Y.S.; Song, S.K. Correlations between pore structure of activated carbon and adsorption characteristics of acetone vapor. *Korean Society of Environmental Engineers* **2005**, *27*, 620–625.
17. Zhang, D.; Jia, D. Toughness and strength improvement of diglycidyl ether of bisphenol-A by low viscosity liquid hyperbranched epoxy resin. *Journal of Applied Polymer Science* **2006**, *101*, 2504–2511.
18. Varley, R.J. Toughening of epoxy resin systems using low-viscosity additives. *Polymer International* **2004**, *53*, 78–84.
19. Bong, C.K.; Kim, Y.G.; Lee J.H.; Bong, H.K.; Kim, D.S. Mutual comparison between two the real-time optical particle counter for measuring fine particles. *Journal of the Korean Society of Urban Environment* **2015**, *15*, 219–226.
20. ISO 12103-1; *Road vehicles-Test dust for filter evaluation-Part 1: Arizona test dust*; International Organization for Standardization: Geneva, Switzerland, 1997.
21. ISO 22197-1; *Fine ceramics (advanced ceramics, advanced technical ceramics) – test method for air-purification performance of semiconducting photocatalytic materials – Part 1: Removal of Nitric Oxide*; International Organization for Standardization: Geneva, Switzerland, 2007.